

北海道・東北日本沈み込み帯における温度構造：スラブの形状と斜め沈み込みの影響
Thermal structure of the NE Japan-Hokkaido subduction system: The effects of 3-D slab geometry and oblique subduction

和田 育子^{1*}; Jiangheng He²; 長谷川 昭³; 田村 芳彦⁴; 中島 淳一³
WADA, Ikuko^{1*}; JIANGHENG, He²; HASEGAWA, Akira³; TAMURA, Yoshihiko⁴; NAKAJIMA, Junichi³

¹ 東北大学災害科学国際研究所, ² パシフィック地球科学センター, ³ 東北大学地震・噴火予知研究観測センター, ⁴ 独立行政法人海洋研究開発機構

¹IRIDeS, Tohoku University, ²Pacific Geoscience Centre, Canada, ³Graduate School of Science, Tohoku University, ⁴Japan Agency for marine-Earth Science and Technology

In this study, we first examine the effects of along-strike variation in slab geometry and oblique subduction on subduction zone thermal structures by comparing 3-D numerical thermal models with a range of generic subduction geometries and parameters with a 2-D reference model. We found that changes in slab dip along a straight margin have modest effects on the mantle flow pattern and thus the thermal field. However, concave and convex ocean-ward margins result in cooler and warmer mantle wedges, respectively, and oblique subduction results in a warmer mantle wedge, compared to the 2-D reference model. We developed a 3-D thermal model for the NE Japan-Hokkaido margin, using a well-constrained 3-D slab geometry model. In general, there is little 3-D effect on the thermal structure of the shallow part (<70 km depth) of the subduction system, where the mantle does not participate in the slab-driven wedge flow. We also found that the 3-D effect is small in the deeper part of the southern half of the system, where the margin is relatively straight and the slab dip does not vary significantly along the margin. These results indicate that 2-D models provide excellent approximations for the thermal structures of the shallow part and the southern part of the subduction system. However, from the northern part of NE Japan to Hokkaido, the mantle flow pattern is affected by the concave ocean-ward margin and oblique subduction, and the wedge is cooler near the NE Japan-Hokkaido junction and warmer in Hokkaido than the 2-D thermal models for the respective regions. We compare the 3-D thermal modeling results with along-strike variations in surface heat flow, arc magma geochemistry, and earthquake distribution in NE Japan and Hokkaido.

キーワード: Tohoku-Hokkaido subduction system, 3-D thermal model, slab geometry, oblique subduction, mantle wedge flow, earthquakes and volcanism

Keywords: Tohoku-Hokkaido subduction system, 3-D thermal model, slab geometry, oblique subduction, mantle wedge flow, earthquakes and volcanism

スラブとマントルがデカップリングする深さの空間変化がスラブ表面温度に与える影響
Effects of a local deepening of slab-mantle decoupling depth on slab surface temperature

森重 学^{1*}; van Keken Peter²
MORISHIGE, Manabu^{1*}; VAN KEKEN, Peter E.²

¹ 独立行政法人海洋研究開発機構, ² ミシガン大学
¹JAMSTEC, ²University of Michigan

In the subduction zone, we generally observe low seismic attenuation in the forearc mantle. In addition, surface heat flow shows low value in the forearc and a sudden transition to high value in the arc. These observations suggest that the forearc mantle is cold and is not involved in the corner flow in the mantle wedge. We can understand it in terms of slab-mantle decoupling depth (D_{dec}). Above D_{dec} , the mantle does not move with the slab just beneath it. Therefore, it becomes cold quickly due to the cooling from the overriding plate and the slab. Below D_{dec} , on the other hand, the mantle moves with the slab. It keeps this part of mantle warm by advection of hot material due to the corner flow. Thus, D_{dec} is a key parameter which strongly affects thermal structure in the subduction zone. Comparison of the observed surface heat flow and the one predicted with 2D numerical model suggests that D_{dec} does not vary much for each subduction zone and is 70-80km, but in each subduction zone D_{dec} may show some degree of along-arc variation. One such example is the junction between Japan and Kurile arcs, where the down-dip limit of thrust type earthquake is locally deepened by around 15km. In this presentation, we investigate the effects of a local deepening of D_{dec} on slab surface temperature.

Toward the goal, we use time-dependent 3D finite element models to compute mantle flow and temperature. Only mantle wedge is treated as a dynamic entity. We use a simple slab geometry and assume a local deepening of D_{dec} to see its effects. We find that the increase in slab surface temperature at D_{dec} is larger where we assume a deepening of D_{dec} , which produces a warmer region there. It is caused by 3D flow in the mantle wedge due to along-arc variation of D_{dec} . We also calculate surface heat flow from obtained thermal structure, but it does not show significant along-arc variation. These results do not change even when we use a realistic slab geometry which is similar to that of the junction between Japan and Kurile arcs. While the surface heat flow anomaly and deepening of the seismic belt in S. Hokkaido cannot be easily explained by these models, the temperature excursions at the slab surface are significant. These models predict potentially strong variations in the conditions that the fluids leave the slab, which may be visible by various new geothermometers, such as those based on the H₂O/Ce ratio.

Keywords: subduction zone, slab-mantle decoupling depth, slab surface temperature

西南日本におけるフィリピン海プレートの沈み込みに伴う温度モデリング Thermal modeling associated with subduction of the Philippine Sea plate in southwest Japan

吉岡 祥一^{1*}; 季 穎鋒¹; 松本 拓己²
YOSHIOKA, Shoichi^{1*}; JI, Yingfeng¹; MATSUMOTO, Takumi²

¹ 神戸大学都市安全研究センター, ² 防災科学技術研究所
¹RCUSS, Kobe University, ²NIED

By constructing a parallelepiped three-dimensional thermal convection model, we investigated temperature, mantle flow and heat flow distributions associated with subduction of the Philippine Sea (PHS) plate in southwest Japan. We proposed new, realistic, and high-resolution temperature field on the plate interface, and attempted to clarify its relationships with the occurrences of megathrust earthquakes, long-term slow slip events (SSE), and low frequency tremors (LFEs). For this purpose, we newly developed a numerical model to deal with subduction of an oceanic plate with 3D arbitrary geometry. We modeled subduction of the PHS plate by using the up-to-date three-dimensional slab geometry, referring to high resolution P-wave seismic tomography and seismic reflection studies. We also used large number of heat flow data such as BSRs, borehole, heat probe, and Hi-net to constrain calculated temperature field, and took account of complicated subduction history in southwest Japan. The results showed that the interplate temperature was lower by approximately 100 °C in western Shikoku where a larger true subduction angle exists than eastern Shikoku. Temperature change due to erosion and sedimentation affected surface heat flow with short wavelength. We also found that the obtained interplate temperature in the Nankai seismogenic zone was wider than that in the Tonankai seismogenic zone. The LFEs occurred near the plate interface with temperatures ranging from 350 °C to 450 °C at depths of 30 to 40 km. The existence of large temperature gradients from the surface to the inside of the PHS plate was considered to be related to the occurrence of long-term slow slip events beneath the Bungo Channel.

Slab-wedge mantle boundary preserved in the Sanbagawa belt, SW Japan Slab-wedge mantle boundary preserved in the Sanbagawa belt, SW Japan

ウォリス サイモン^{1*}; 森 宏¹; 永治 方敬¹; 河原 弘和¹

WALLIS, Simon^{1*}; MORI, Hiroshi¹; NAGAYA, Takayoshi¹; KAWAHARA, Hirokazu¹

¹Dept. Earth & Planetary Sci., Nagoya Uni.

¹Dept. Earth & Planetary Sci., Nagoya Uni.

The Sanbagawa belt of SW Japan is a high-pressure low-temperature subduction type metamorphic belt. The rock types consists of mafic, siliceous and pelitic schists derived from the subducted slab. There are also a series of ultramafic bodies whose origin is disputed: both a slab and wedge mantle origin have been proposed. However, the clear relationship between the distribution of the mantle rocks and metamorphic grade provides strong evidence that they were derived from the wedge mantle. We carried out a detailed study of the Shiragayama body as an example of serpentized mantle from close to the corner of the wedge. Studies of this region can contribute to our understanding of non-volcanic tremor and fluid flow that occurs in these otherwise inaccessible parts of subduction zones.

Keywords: fore arc mantle, subduction metamorphism, slab mantle boundary

Phenomenology of Episodic Tremor and Slip Phenomenology of Episodic Tremor and Slip

小原 一成^{1*}
OBARA, Kazushige^{1*}

¹Earthquake Research Institute, UTokyo

¹Earthquake Research Institute, UTokyo

Episodic Tremor and Slip (ETS) is a coupling phenomenon composed of continuous weak seismic events and geodetic short-term slow slip event (SSE) in the transition zone between the brittle seismogenic zone and stable sliding regime recognized in southwest Japan and Cascadia. This paper reviews characteristics of ETS and related phenomena to contribute to discussion for subduction process.

ETS is interpreted as a stick slip on the plate interface accompanied by seismic swarm at small patches surrounded by the SSE plane because of coincidence of their sources and linear relationship between the duration of tremor episode and the moment of SSE estimated geodetically for each episode. ETS is distributed in a narrow belt-like zone along the strike of the subducting plate. ETS zone is divided into several segments in which episodes recur at each regular recurrence interval. However ETS is not "characteristic earthquake" because the rupture area and recurrence interval are fluctuated. Sometimes we observe rupture propagation through a couple of segments. The segment is usually bounded by gap which is considered as not a barrier but an easily sliding portion because of the existence of multi-segment migration.

ETS activity has depth dependent property. At the deeper part of the ETS zone minor episode frequently occurs, on the other hand major episode occurs infrequently at the shallower part. Large ETS usually initiates from the deeper part and migrates upward then activates at the shallower part. This might be caused by gradual change in frictional property with increasing the depth. At the downdip edge of the ETS zone tremor episode easily occur due to weak strength and stress concentration from stable sliding zone. Each small episode transfers the stress to the updip side. Finally a small episode can propagate to the updip edge then develop as a large ETS episode.

The activity style of ETS in southwest Japan and Cascadia is very similar; however there are some differences. One is the existence of deep very low frequency earthquake (VLF). In Japan the VLF earthquake is usually associated with ETS but has not been detected in Cascadia. It might depend on the detection capability or difference in inhomogeneity of the plate interface because the distribution of VLF earthquake in southwest Japan is more localized compared to that of tremor.

The other difference is the existence of long-term SSE. It is detected at the updip side of ETS zone in the Bungo Channel and Tokai in southwest Japan but not detected in Cascadia. The long-term SSE with duration from several months to years activates tremor at the adjacent limited region in the ETS zone. On the other hand, the tremor activity at the downdip part is not affected. Similar long-term SSE has been detected in Alaska and Mexico, where tremor activity was recently detected at the downdip side of the source fault of the long-term SSE. The tremor is seems to be activated during the SSE period like as in southwest Japan. The long-term SSE in Tokai is located above the anomalously high V_p/V_s region in the slab. In Mexico, a ultra slow speed layer was found in the long-term SSE source region. Therefore, the anomalous structure might be a cause of the long-term SSE. ETS and long-term SSE are quite different in the slip velocity. It might reflect the difference in the frictional property. In Tokai, the source region of the long-term SSE and ETS is bounded by the inland Moho discontinuity. Therefore, ETS occurs at the interface between the subducting plate and overlying mantle wedge.

ETS has not been recognized besides in southwest Japan and Cascadia; however ambient tremor has been detected in some regions. We expect that the ambient tremor is triggered by small SSE which is not detected by the current observation. Understanding detail relationship between tremor and SSE based on improvement detection capability is important to reveal the mechanism of ETS.

Keywords: slow earthquake, non-volcanic tremor, slow slip event, subduction zone, plate interface

Enhancement of slow earthquakes by geometrical irregularity of subducting oceanic crust Enhancement of slow earthquakes by geometrical irregularity of subducting oceanic crust

加藤 愛太郎^{1*}; 小原 一成¹; 武田 哲也²
KATO, Aitaro^{1*}; OBARA, Kazushige¹; TAKEDA, Tetsuya²

¹ 東京大学地震研究所, ² 防災科学技術研究所
¹ERI University of Tokyo, ²NIED

Along the worldwide subduction zones, slow earthquakes commonly occur on the deep extension of major tectonic boundary which hosts megathrust earthquake rupture. Slow earthquakes silently release stress to the adjacent seismogenic zone, raising the likelihood of promoting unstable fast slip. However, what controls the transitional variations in fault-slip behaviors from fast to slow modes on the deep extension of megathrust fault remains controversial. Here we use a high-resolution receiver function and seismic tomography illustrated by dense seismic arrays to analyze the structural elements in the subduction complex and fore-arc mantle wedge beneath the Shikoku Island, Japan, where episodic tremor and slow-slip events (ETS) have been most intensive for over a decade.

We find out that deformed oceanic crust with irregularity of surface geometry horizontally lies in the ETS zone, where low seismic velocity zone with high Poisson's ratio that we interpret as high pore-fluid pressure. Step-like discontinuous alignments of intra-slab seismicity support the flat-subduction of the oceanic crust with faulting structure. In contrast, at depths shallower than the ETS zone, the low velocity anomaly within the oceanic crust is weak and dipping towards the NW, implying less amount of high-pressured fluid in the tilting oceanic crust. In addition, lithology of the overlying plate changes to partially serpentinized mantle wedge in the ETS zone. Locally flat-geometry of the subducting oceanic crust combined with the contact of serpentine enhances accumulation of high-pressurized fluids along the plate interface, leading to segregation between slow and fast slip modes at the deep transition zone of mega-thrust fault.

蛇紋岩の高温高圧変形実験によるスロー地震発生機構に関する考察 Deformation experiments on serpentinite at high PT conditions with implications for the mechanisms of slow earthquakes

岡崎 啓史^{1*}; Hirth Greg¹; Proctor Brooks¹; 片山 郁夫²; 高橋 美紀³
OKAZAKI, Keishi^{1*}; HIRTH, Greg¹; PROCTOR, Brooks¹; KATAYAMA, Ikuo²; TAKAHASHI, Miki³

¹Department of Geological Sciences, Brown University, ² 広島大学大学院理学研究科地球惑星システム学専攻, ³ 産業技術総合研究所

¹Department of Geological Sciences, Brown University, ²Department of Earth and Planetary Systems Science, Hiroshima University, ³Geological Survey of Japan, AIST

To understand the spatial and temporal distribution of earthquakes and deformation in subduction zones, it is important to constrain the rheological properties of metamorphic rocks (i.e., altered mantle, oceanic crust and sediments), and how they evolve during metamorphic reactions following hydration, carbonation and dehydration of the down-going slab. Especially, antigorite (the high-temperature serpentine polytype) serpentinite, the dominant metamorphic phase in hydrated mantle material at the condition of mantle wedge, is the key metamorphic rock to understand the generation mechanism of slow earthquakes and slab-mantle coupling at the plate interface in subduction zones.

Deformation experiments on antigorite serpentinite were conducted within and above the thermal stability field of antigorite using a gas pressure-medium apparatus and a solid pressure-medium apparatus to understand how dehydration reactions influence the mechanical behavior of antigorite serpentinite. At 400 °C, within the stability field of antigorite, antigorite serpentinite shows stable sliding and a positive velocity dependence of shear stress (i.e., friction coefficient). Shear stress increased with increasing confining pressure, while the friction coefficient decreases from 0.55 to 0.37 with increasing confining pressure from 200 MPa to 1500 MPa. These results indicate that antigorite serpentinite deforms by brittle and semi-brittle processes in subduction zones.

During the experiments using a gas pressure-medium apparatus at a confining pressure of 200 MPa and temperatures close to the dehydration temperature of antigorite (450-550 °C), antigorite serpentinite shows a slow stick-slip behaviour, which is characterised by relatively long durations and small stress drops during slip, while this type of behaviour was not observed at higher temperatures when the antigorite becomes completely dehydrated. Stick-slip in this temperature range is consistent with the temperature range where slow earthquakes occur at the corner of the mantle wedge in southwest Japan and Cascadia. The scaling law of slow stick-slip in the antigorite serpentinite gouge is distinct from that of regular earthquakes and a theoretical duration estimated from the apparatus stiffness, but similar to that of slow earthquakes.

We also conducted deformation experiments in which temperature was increased above the thermal stability of antigorite to simulate a prograde metamorphism in subduction zones, similar to the experiments by Chernak and Hirth (2011) but with a general-shear geometry. With increasing temperature from 400 °C to 700 °C during deformation, differential stress decreased and reached 120 MPa. Recovered sample suggest that the strain localizes within shear fractures and limited dehydration occurred during the experiments.

These results suggest that the dehydration of antigorite can form weak zones within the mantle wedge along the plate interface in subduction zones, even if the extent of the dehydration reaction is limited. In addition, slow instabilities of the slip interface can be caused by the dehydration of antigorite within the weak zone in the antigorite serpentinite layer, which can result slow earthquakes.

Keywords: antigorite, serpentinite, semi-brittle flow, slow earthquakes, dehydration, hydrothermal condition

交代作用を伴う沈み込みプレート境界断層の弱化 Metasomatic fault-zone weakening of subduction plate boundary faults

平内 健一^{1*}; スパイアーズ クリストファー²
HIRAUCHI, Ken-ichi^{1*}; SPIERS, Christopher²

¹ 静岡大学, ² ユトレヒト大学

¹Shizuoka University, ²Utrecht University

Fluid influx along faults triggers stress-induced dissolution and precipitation processes, leading to syntectonic growth of weak phyllosilicates. In subduction zones, slab-derived Si-rich fluids may infiltrate into the forearc wedge and transform primary mantle minerals into hydrous phases such as serpentines and talc, changing the mechanical and seismogenic properties of subduction plate boundary faults. However, it remains unclear how frictional strength and sliding stability of the plate boundary faults evolve via Si-metasomatism.

Hirauchi et al. (2013, *Geology*) performed frictional sliding experiments on antigorite (70%) plus quartz (30%) gouges at a pore fluid pressure (P_f) of 200 MPa, an effective normal stress (σ_{eff}) of 200 MPa, temperatures (T) of 20, 300, 400, and 500 °C, and sliding velocities (V) of 0.1-30 $\mu\text{m/s}$, using a hydrothermal ring shear machine. At temperatures of 300-500°C, the gouges exhibited a peak friction coefficient (μ) of 0.40-0.62, followed by strain weakening towards a quasi-steady-state μ of 0.25-0.47. The weakening was mainly due to the development of through-going, talc-rich boundary shears. The steady-state μ of the gouges decreased systematically as the talc-rich layer widened.

At central California, there are several boundary faults that separate serpentinite bodies from shale-matrix melanges of the Franciscan accretionary complex. The serpentinite body is overprinted by anastomosing development of crack-seal veins of talc, serpentine, and calcite, suggesting that intense water-rock interaction took place in connection with faulting. The serpentinite along the faults represents a cataclastic shear zone that records brittle deformation, consisting of angular fragments that are suspended in fine-grained, randomly-oriented talc matrix. Frictional sliding experiments conducted at $P_f = 40, 80, \text{ and } 120$ MPa, $\sigma_{eff} = 60, 120, \text{ and } 180$ MPa, $T = 20, 150, \text{ and } 300$ °C, and $V = 0.3-100$ $\mu\text{m/s}$ showed that the serpentinite has friction coefficients that agree with Byerlee's law (μ 0.6), while the cataclasite is much weaker with friction coefficients as low as 0.2. Examination of the velocity dependence of friction revealed that the serpentinite exhibits both velocity-weakening and velocity-strengthening behavior, whereas the cataclasite is velocity strengthening under all conditions investigated.

Our results demonstrate that in the lowermost part of the forearc wedge, where silica-saturated fluids infiltrate from the dehydrating slab, metasomatically produced talc will form in the intensely sheared serpentinite, causing a much larger weakening effect than expected for serpentines, even if the total amount of talc formed is minor (<10 vol%). The continued reaction with Si-rich fluid will also result in a transition from seismic to aseismic behavior of the plate boundary faults.

キーワード: 沈み込み帯, 蛇紋岩, 交代作用, 断層

Keywords: subduction zone, serpentinite, metasomatism, fault

水熱実験からみるマントル-地殻境界における物質移動と蛇紋岩化作用のカップリング Coupled mass transport and serpentinization at crust/mantle boundary: Insights from hydrothermal experiments

岡本 敦^{1*}; 大柳 良介¹; 土屋 範芳¹
OKAMOTO, Atsushi^{1*}; OYANAGI, Ryosuke¹; TSUCHIYA, Noriyoshi¹

¹ 東北大学大学院環境科学研究科

¹ Graduate School of environmental Studies, Tohoku University

Serpentinization commonly proceeds by a supply of water passing through crust, and thus a large mass transport could occur during serpentinization reactions. Especially, silica activity is known as a control of the reaction paths and rate during the hydrothermal alteration of peridotites [1, 2]. However, it is still unclear the role of mass transport on reaction paths, overall hydration rate and volume change during serpentinization. In this study, we conducted two types of hydrothermal experiments on serpentinization. First one is the metasomatic-reaction experiments between olivine (Ol) + quartz (Qtz) zones as analogue of boundary of mantle and crustal rocks. Second one is the hydrothermal experiments with sintered olivine (analogue of low porosity rock). Both types of experiments were carried out at 250 °C and vapor-saturated pressure (= 3.98 MPa) in alkaline aqueous solution.

In the Ol-Qtz metasomatic experiments (up to 46 days.), composite powders, which was composed of Qtz zone and Ol zone was set in inner tubes and then loaded into autoclave. After the experiments, the mineralogy and H₂O content of the products were evaluated as a function of the distance from Ol/Qtz boundary. The reaction products after olivine are serpentine (Srp), brucite (Brc), magnetite (Mgt) and smectite (Smc) (instead of talc). The products systematically change from the Smc+Srp to Srp+Brc+Mgt with increasing the distance from the Ol/Qtz boundary. The H₂O content of the products is low at the Ol/Qtz boundary (i.e., 3.9 wt.% after 46 days), and increases toward the margin of the tube (12 wt.% at ~30 mm from the Ol/Qtz boundary).

The detailed mass balance calculation between 25 to 46 days reveals the characteristic nature of the metasomatic reactions and porosity change as follows. Near Ol/Qtz boundary (Smc+Srp zone), smectite was formed by supply of silica in two ways; hydration of olivine and dehydration of serpentine. In contrast, at the zone far from the boundary (Srp+Brc zone; >20 mm from O/Qtz), the production rate of serpentine and brucite are constant without any silica supply. At the transition zone between Smc+Srp and Srp+Brc zones, a large amount of serpentine is formed by consumption of both brucite and olivine, which results in a largest porosity reduction (~30 %). In the Smc+Srp zone, dehydration and porosity reduction occurs simultaneously, implying a possible raise of fluid pressure. Silica metasomatic reactions causes a significant variation not only in mineral assemblage but also in porosity and fluid pressure, which will characterize the dynamic change of mechanical properties at crust/mantle boundary.

In the hydrothermal experiments of the sintered olivine, the starting olivine aggregate (initial porosity <~10 %, covered by Pt jacket), which was made by hot press at 1200 degreeC, 1 GPa and 4 days, was emplaced in the alkaline water. After 3 days, we recognized the progress of serpentinization reaction to produce serpentine and brucite. An interesting finding of this experiment is that brucite did not formed in pores of the core sample, but it was formed only at the top of the cylindrical core of the sample. This result is quite different from with our previous experiments with using olivine powder (initial porosity is ~50 %) [3], in which brucite and serpentine was formed uniformly. The result of our present study of the sintered olivine suggests that, when the rock porosity is low and volume expansion is difficult, brucite is segregated into open space (c.a. open fracture) during serpentinization; which may also affects on the formation of the local weak zone within the mantle peridotite.

[1] Frost, B. R., & Beard, J. S., 2007. *Journal of Petrology*, 48, 1351-1368.

[2] Ogasawara, Y., Okamoto, A., Hirano, N., & Tsuchiya, N., 2013. *Geochim. Cosmochim. Acta*, 119, 212-230.

[3] Okamoto, A., Ogasawara, Y., Ogawa, Y. and Tsuchiya, N., 2011. *Chemical Geology*, 289, 245-255.

Keywords: serpentinization, hydrothermal experiments, silica metasomatism, porosity change, hydration, mass transport

西南日本の沈み込み帯メランジュ中のヒスイ輝石岩に記録された塩水 Saline fluids recorded in jadeitites in subduction-zone melanges of southwest Japan

森 康^{1*}; 重野 未来¹; 川本 竜彦²; 西山 忠男³

MORI, Yasushi^{1*}; SHIGENO, Miki¹; KAWAMOTO, Tatsuhiko²; NISHIYAMA, Tadao³

¹北九州市立自然史・歴史博物館, ²京都大学地球熱学研究施設, ³熊本大学自然科学研究科

¹Kitakyushu Mus. Nat. Hist. Hum. Hist., ²Inst. Geotherm. Sci., Kyoto Univ., ³Grad. Sch. Sci. Tech., Kumamoto Univ.

Slab-derived fluids play essential roles in mass transfer along subduction-zone channels between the subducting slab and mantle wedge (e.g., Bebout 2013 Metasomatism and the chemical transformation of rocks; Spandler and Pirard 2013 Lithos). Salinity of such slab-fluids probably affects solubility and fluid-rock partitioning of elements; therefore, it remains to be investigated in various rocks. Jadeitite is a rock composed mainly of jadeite (sodium pyroxene, NaAlSi₂O₆) and occurs typically in serpentinite mélanges intercalated to high-pressure and low-temperature metamorphic belts. This curious rock is thought to be the product of direct precipitation from aqueous fluids and/or of fluid-induced metasomatism of a protolith (Harlow *et al.* 2007 Geology of gem deposits, Tsujimori and Harlow 2012 Eur J Mineral, and references therein). Fluid inclusions are commonly observed in jadeitites, and they may provide information about the fluid composition in subduction-zone mélanges. We determined major components and salinity of fluid inclusions in the jadeitites collected from eight localities in Japan: Omi-Itoigawa (Omi-Renge belt), Oya and Osa (Suo belt), Kochi (Kurosegawa belt), Mie and Tone (Nishisonogi metamorphic rocks), and Shimonita and Yorii (the origin unclear). In all of the studied rocks, primary fluid inclusions consist of a liquid phase and a gas bubble. Raman spectra show the presence of H₂O liquid and vapor with or without minor CH₄ gas. The freezing point of the liquid phase indicates high-salinity (up to 8 wt% NaCl equivalent) of the primary fluid inclusions. The salinity varies among the localities of the jadeitite. For example, the salinity of the primary fluid inclusions is about 7.1 ± 0.1 wt% NaCl equivalent in the albite jadeitite from Oya and about 4.6 ± 1.2 wt% NaCl equivalent in quartz inclusions bearing jadeitite from Tone. Some jadeitite samples contain secondary CH₄-rich fluid inclusions along healed microcracks. The presence of minor CH₄ is also reported in the saline fluids inclusions with 5.1 ± 1.9 wt% NaCl equivalent from the Myanmar jadeitite (Shi *et al.*, 2005 Geochem J). The present findings suggest that saline fluids with or without CH₄ are common in subduction-zone mélanges in Japan as well as in Myanmar. The reduced conditions can be caused by serpentinitization processes. This is contrast to the CO₂-bearing saline fluids in the peridotite xenoliths from fore-arc mantle wedge (Kawamoto *et al.*, 2013 PNAS). The high-salinity of the slab-fluids probably enhances the mobility of elements such as Pb in subduction-zone channels (Keppler, 1996 Nature, Shigeno *et al.*, 2012 Eur J Mineral).

キーワード: 塩水, ヒスイ輝石岩, 流体包有物, 蛇紋岩メランジュ, 沈み込み帯

Keywords: saline fluid, jadeitite, fluid inclusion, serpentinite mélange, subduction zone

沈み込み境界上盤の蛇紋岩構造：三波川帯の天然の例 Serpentinite structure above subduction surface: Analysis of a natural example in Sanbagawa metamorphic belt

水上 知行^{1*}; 曾田 祐介¹; 横山 寛紀¹; 平松 良浩¹

MIZUKAMI, Tomoyuki^{1*}; SODA, Yusuke¹; YOKOYAMA, Hironori¹; HIRAMATSU, Yoshihiro¹

¹ 金沢大学

¹ Kanazawa University

Serpentinization is a key reaction in forearc mantle. Formation of strong schistosity and shear zones under high differential stresses provides anastomosing networks of fluid pathways as well as seismically anisotropic nature in the mantle. Understanding of such structural development is important for both interpretation of seismic analyses and forward modelling of subduction system including thermal structure, material circulation, magma process and slip behaviours of subduction boundaries.

We report results of petrological and structural analyses of layered antigorite (Atg) serpentinite in the marginal part of the Higashi-akaishi ultramafic unit in the Sanbagawa belt. This is a product of hydration of dunite (a rock consisting of almost 100% olivine (Ol)) due to metamorphic fluid from the underlying meta-sediments and meta-basites. Strong shape preferred orientation of Atg and existence of boudinaged layers indicate fluid-rock reaction under extensional deformation.

The layered structure is defined by a centimeter to meter-scale interlayering between Ol-rich and Atg-rich units. The modal amounts of Atg in these units form peaks at 15 vol% and 50 vol%, respectively, showing a bi-modal distribution as a whole. Effects of initial microstructures on the extent of serpentinization are limited: Porphyroclastic and fine-grained dunite, that occupy a large part of the outcrop, are transformed to both Ol-rich and Atg-rich layers although dunite with more than 50% of coarse Ol grains has been poorly serpentinized. Each Atg layer shows millimeter-scale spaced foliations defined by amounts of Ol and Atg and locally shows a diffusive variation in millimeter to centimeter-scales. Thickness and proportion of Atg-rich layers increase near the contact with crustal rocks.

Reaction for the Atg formation is constrained based on re-distribution of elements among Ol, Atg and opaque minerals. As serpentinization proceeds, Ol is enriched in Fe and Ni owing to their incompatibility in Atg. Taking concomitant formations of minor amounts of magnetite and sulfides into account, the variation of the Ol composition and modal amounts of serpentinization products are quantitatively explained by the following reaction: $\text{Ol} + \text{SiO}_{2,aq} + \text{H}_2\text{O} \Rightarrow \text{Atg}$. This indicates that the development of Atg has been controlled by a supply of silica in aqueous fluids.

We measured thickness of 70 layers for each and, taking the layers with the thickness lower than 200 centimeters, we found exponential relationships in cumulative frequency distributions both for Ol-rich and Atg-rich layers. Relative thickness between neighbouring units $[d(\text{Ol})/d(\text{Atg})]$ also shows an exponential distribution. We could not find any regular relationships among width and spacing like Liesegang patterns.

It is known that pattern structures appear in reaction-diffusion systems. The above observations strongly suggest that the development of layered structures in Atg serpentinite is controlled by interaction between reaction and material transfer. In this case, potential causes of heterogeneous serpentinization may be diffusional contrast between H_2O and SiO_2 or permeability contrast between Ol-rich and Atg-rich layers. Scaling analyses of deep low frequency tremors showed that duration-amplitude and size-frequency distributions of tremors in SW Japan can be fit with exponential models rather than power-law models. The seismological observations imply structural heterogeneity with unique scale length. Further examination on the exponential relationships developed in serpentinite may contribute to understand the slip phenomena on plate interfaces.

Keywords: serpentinite, layered structure, reaction-diffusion, exponential frequency distribution, deep low frequency tremor

福島県大島半島に産する蛇紋岩中のアワルワ鉱 Awaruite in serpentinites from Oshima Peninsula, Fukui Prefecture, Japan

山口 海^{1*}; 上原 誠一郎²
YAMAGUCHI, Kai^{1*}; UEHARA, Seiichiro²

¹九州大学大学院理学府地球惑星科学専攻, ²九州大学大学院理学研究院地球惑星科学部門

¹Department of Earth and Planetary Sciences, Faculty of Science, Kyushu University, ²Department of Earth and Planetary Sciences, Faculty of Science, Kyushu University

Awaruite is one of native Ni-Fe alloys, and the compositional range is Ni₂Fe to Ni₃Fe. The space group is *Fm3m* or *Pm3m* (e.g., Williams, 1960; Ahmed et al., 1981). Typical grain sizes are 10-300 μm, and grain shapes are typically irregular, anhedral or skeletal. It is found only in the serpentinized peridotites and chondritic meteorites (e.g., Ramdohr, 1967; Clarke et al., 1970). In general, awaruite is observed in serpentine vein (Sakai and Kuroda, 1983), and coexist with other metal minerals (Kanehira et al., 1975). This study deals with the characteristic occurrence of awaruite in pseudomorph texture in the Oshima serpentinites from Oshima peninsula, Fukui prefecture, Japan.

All samples were examined with polarizing microscope observation, X-ray diffraction analysis and SEM-EDS analyses. Preparation of TEM specimen and microtexture observation were conducted with an ion milling machine (JEOL EM-09100IS) and TEM (JEOL JEM-2000FX, JEM-3200FSK) in the Research Laboratory for High Voltage Electron Microscopy (HVEM), Kyushu University, Japan. Chemical analyses of microtexture were also examined using JEM-3200FSK equipped with EDS.

Peridotites in this area are partially or perfectly serpentinized. Texture of the serpentinite is mesh texture after forsterite and vein texture. Scarcely serpentinized enstatite is also observed. Each mesh texture is composed of mesh rim shows optical anisotropy and mesh core shows optical isotropy. The serpentinization of mesh texture is strong in close to vein textures. Most mesh rims near vein texture consist of some layers; outer rim, outer-inner rim boundary and inner rim. These rims consist of chrysotile, about 50 nm in width and 2 μm in length, and lizardite, about 300 nm in width and 1 μm in length, and outer-inner rim boundary about 2 μm in width are filled with serpentine fine grains, up to 100 nm in diameter.

A number of awaruite fine grains, 200-300 nm diameter, array along cell boundary, outer-inner rim boundary and rim-core boundary. These awaruite coexist with no other metal minerals; pentlandite, magnetite and etc. In contrast, metal minerals in vein texture are magnetite and minor pentlandite. These results indicate that mesh texture in serpentinite is extremely reductive environment compared with vein texture. The chemical composition of awaruite (average of four analysis) is Ni 73.13% and Fe 26.87%. The cross-section of these awaruite grains is square or rhombic, indicating that these grains are cube or octahedral crystals (fig. 1a). These grains seem to be euhedral from grain shapes, and this is characteristic compared with previous studies (e.g., Rubin, 1991). The SAED pattern recorded along the [001] zone axis shows strong 200, 220 reflections and weak 100, 110 reflections (fig. 1b). This indicates space group of the Oshima awaruite is *Pm3m*, which is ordering phase of *Fm3m* awaruite. Lower symmetry of the Oshima awaruite will be formed lower temperature.

キーワード: アワルワ鉱, 網目状組織, 蛇紋岩, 微細組織, 蛇紋石鉱物, 透過電子顕微鏡

Keywords: Awaruite, Mesh texture, Serpentinite, Microtexture, Serpentine minerals, TEM

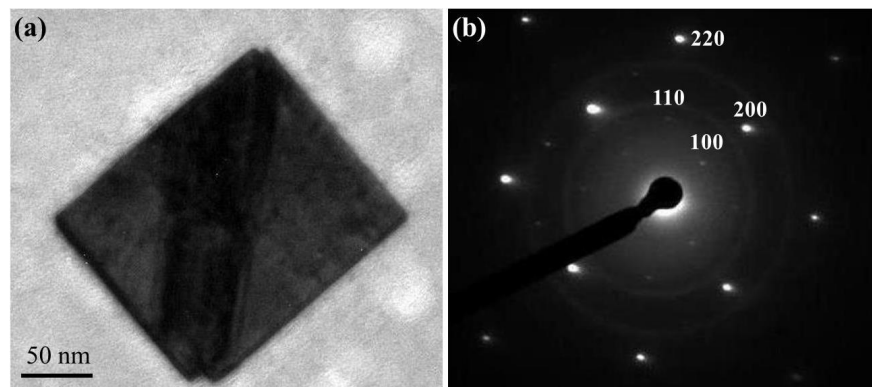


Fig. 1. (a) TEM image of awaruite in mesh texture. (b) The SAED pattern of (a) recorded along the [100] zone axis.

アンチゴライト CPO の測定 Antigorite CPO measured by U-stage, EBSD and synchrotron X-rays

曾田 祐介^{1*}; 安東 淳一²; 浦田 義人²; Wenk Hans-Rudolf³
SODA, Yusuke^{1*}; ANDO, Jun-ichi²; URATA, Yoshito²; WENK, Hans-rudolf³

¹ 金沢大学, ² 広島大学, ³ カリフォルニア州立大学

¹Kanazawa University, ²Hiroshima University, ³University of California, Berkeley

Foliated antigorite serpentinite with crystallographic preferred orientation (CPO) probably causes shear wave splitting observed at subduction zones (e.g., Katayama et al., 2009). Therefore, the study of type and intensity of antigorite CPO is an important to understand the detail of this phenomenon.

Soda and Wenk (2014) measured CPOs of antigorite serpentinite from the Sashu Fault at the Saganoseki Peninsula, Oita Prefecture, by three independent methods, U-stage (with optic microscope), EBSD and synchrotron X-rays. The obtained antigorite CPOs by three methods are almost same without the fabric strength, maxima of pole figures in multiples of random distribution. The fabric strength decreases in the following order, U-stage >EBSD >synchrotron X-rays, which is probably caused by the characteristics of three methods. Through U-stage measurement, we can obtain the fabric pattern of antigorite CPO mainly from coarser antigorite grains (>30 μm). In the case of EBSD measurement, we measure antigorite CPO within an area of ca. 0.8 mm \times 0.8 mm. Measurement points of only ca. 30% can be used to make fabric patterns. Residual ca. 70% points are neglect, because the quality of Kikuchi lines from them is too low to identify the orientation. In the synchrotron X-rays method, the result represents the bulk fabric from a volume of ca. 0.5 mm \times 0.5 mm \times 1.0mm.

The serpentinite measured antigorite CPO develops mylonitic structures with a penetrative foliation and lineation (Soda and Takagi, 2010). The antigorite grains show undulose extinction. And their grain boundary is unclear under the microscopy. Mg# (Mg/(Mg+Fe)) of antigorite grains is wide range 0.98-0.88. The BSE images indicate Fe-rich antigorite infilling the grain boundaries and fractures of Mg-rich antigorite.

The same serpentinite has already observed by TEM (Urata et al., 2009). The results indicate that the m-values of antigorite grains, the number of octahedral along the [100] modulation wave, make two groups, high m-value (16-18) and low m-value (13-14). This result suggests that the antigorite are crystallized mainly two stages, which is supported by the variation of Fe contents of antigorite (Fe-rich and Mg-rich). The Mg-rich antigorite grains are main minerals composed of the serpentinite, Fe-rich antigorite grains occupy at the periphery of the others and within the vein. The TEM observation indicates that the Mg-rich antigorite grains are subdivided into sub-grain with 50-100 nm in size, which can be recognized as an undulose extinction under optic microscope.

These microstructures of antigorite grains potentially influence the outcome of CPO measurements. The weaker fabric patterns from the synchrotron X-rays are probably attributed to the fine-grained antigorite crystallized at the deferent stages and to sub-grain. And the U-stage and EBSD measurements focus only the selected grains, which may result in overestimation of elastic wave anisotropy of serpentinite.

References

- Katayama et al, 2009, Nature 461, 1114-1117.
- Soda and Takagi, 2010, Journal of Structural Geology 32, 792-802.
- Soda and Wenk, 2014, Tectonophysics, in press
- Urata et al., 2009, AGU2009 abstract. MR41A-1858.

キーワード: アンチゴライト, CPO, シンクロトロン X 線, 弾性波異方性
Keywords: antigorite, CPO, synchrotron X-ray, elastic anisotropy

Olivine CPO in non-deformed peridotite due to topotactic replacement of antigorite Olivine CPO in non-deformed peridotite due to topotactic replacement of antigorite

永治 方敬¹; ウォリス サイモン^{1*}; 小林 広明¹; 道林 克禎²; 水上 知行³; 瀬戸 雄介⁴; 三宅 亮⁵; 松本 恵⁶
NAGAYA, Takayoshi¹; WALLIS, Simon^{1*}; KOBAYASHI, Hiroaki¹; MICHIBAYASHI, Katsuyoshi²; MIZUKAMI, Tomoyuki³
; SETO, Yusuke⁴; MIYAKE, Akira⁵; MATSUMOTO, Megumi⁶

¹Department of Earth and Planetary Sciences, Nagoya Nagoya University, ²Institute of Geosciences, Shizuoka University, ³Department of Earth Science, Kanazawa University, ⁴Department of Earth and Planetary Science, Kobe University, ⁵Department of Earth and Planetary Science, Kyoto University, ⁶Center for Supports to Research and Education Activities, Kobe University
¹Department of Earth and Planetary Sciences, Nagoya Nagoya University, ²Institute of Geosciences, Shizuoka University, ³Department of Earth Science, Kanazawa University, ⁴Department of Earth and Planetary Science, Kobe University, ⁵Department of Earth and Planetary Science, Kyoto University, ⁶Center for Supports to Research and Education Activities, Kobe University

Olivine crystallographic preferred orientation (CPO) is thought to be the main cause of seismic anisotropy in the mantle, and its formation is generally considered to be the result of plastic deformation of mantle by dislocation creep. Olivine CPO has been reproduced in laboratory deformation experiments and considerable success has been achieved in understanding the deformation conditions (e.g. stress, temperature and water content) under which different olivine CPO patterns develop. This opens the possibility of mapping conditions in the mantle using seismic anisotropy and has been the subject of considerable study. Here we report an alternative mechanism for olivine CPO without the need for deformation. This process may be important in understanding the seismic properties of mantle in convergent margins.

Metamorphic studies show peridotite in the Happo area, central Japan, formed by the dehydration of antigorite-schist related to contact metamorphism around a granite intrusion. Both field and microstructural observations suggest the olivine has not undergone strong plastic deformation. This was confirmed by TEM work that shows the olivine has very low dislocation densities and lacks low angle tilt boundaries. Such tilt boundaries are general stable even after annealing. These features show that peridotite in the Happo area formed in the absence of solid-state deformation.

The olivine of the Happo peridotite formed dominantly by the dehydration breakdown of antigorite schist. We propose that the olivine CPO formed as a result of topotactic replacement of antigorite by the newly formed olivine. EBSD measurements in samples where both antigorite and new olivine are present and in contact show a very close crystallographic relationship between the two minerals: the *a*-axes are parallel, and the *b*- and *c*-axes are perpendicular. We conclude the strong olivine CPO in the Happo area was inherited from the original CPO of the antigorite. Such a process is likely to also occur in subduction zones where serpentinite is dragged down by plate movement. Topotactic growth of olivine may be an important cause of mantle anisotropy in convergent margins.

キーワード: subduction zones, microstructure, B-type olivine CPO, antigorite, topotaxy
Keywords: subduction zones, microstructure, B-type olivine CPO, antigorite, topotaxy

Cr-rich olivine in deserpentinized peridotite and its implication Cr-rich olivine in deserpentinized peridotite and its implication

遠藤 俊祐^{1*}

ENDO, Shunsuke^{1*}

¹産総研 地質情報

¹Institute of Geology and Geoinformation, AIST

Formation of Cr-rich olivine ($\text{Cr}_2\text{O}_3 > 0.1 \text{ wt } \%$) in the presence of Cr-spinel \pm pyroxene has been thought to require extremely reducing and/or high-temperature conditions. Indeed, terrestrial olivine is Cr-free except for some high-T occurrences from Archaean komatiites, inclusions in diamonds, and ultrabasic pseudotachylytes. Deserpentinization is an important fluid release process in subduction zones. One of the best studied examples of this process occurs in Cerro del Almirez (SE Spain), where the antigorite-out reaction front ($\text{Atg} = \text{Ol} + \text{Opx} + \text{Chl} + \text{H}_2\text{O}$) at eclogite facies conditions is well preserved. Large elongate olivine crystals (similar to spinifex textures in komatiites) at the reaction front contain abundant exsolution lamellae of Cr-magnetite, and estimated primary compositions of the elongate olivine show high Cr content (0.1-0.4 wt% Cr_2O_3), leading to a proposal of the spinifex-like textured peridotite being pseudotachylyte ($> 1600 \text{ }^\circ\text{C}$, Evans & Cowan, 2012), in contrast to the generally held view that the elongate olivine crystallized under ambient subduction-zone T ($\sim 680 \text{ }^\circ\text{C}$ at 1.9 GPa) but high supersaturation conditions.

To better understand the dehydration process of serpentinite in subduction zones, this study focuses on a deserpentinized peridotite from the Eclogite unit of the Sanbagawa belt (SW Japan). It consists of porphyroblastic olivine ($\sim 70 \text{ vol } \%$, $\text{Mg}\# = 0.952 \pm 0.004$, $\text{NiO} = 0.37 \pm 0.04 \text{ wt } \%$), antigorite ($\text{Al}_2\text{O}_3 = 0.3\text{-}0.5 \text{ wt } \%$), brucite, zoned Cr-spinel and Ni sulfides. Olivine porphyroblasts contain inclusions of antigorite, brucite, magnetite and Ni sulfides, suggesting that the olivine-forming reaction $\text{Atg} + \text{Brc} = \text{Ol} + \text{H}_2\text{O}$ took place after serpentinization of a dunitic protolith. Sporadic occurrences of Ni-rich olivine (up to 8.1 wt% NiO) within the olivine porphyroblasts suggest prograde breakdown of Ni-rich sulfides. Zoned Cr-spinel grains are composed of a chromite core, a ferritchromite mantle, and an irregular-shaped overgrowth of Cr-magnetite. The chromite core, being the only primary mineral preserved, shows Cr-rich/Ti-poor compositions [$\text{Cr}/(\text{Cr}+\text{Al}) = 0.74\text{-}0.76$, $\text{TiO}_2 < 0.14 \text{ wt } \%$] indicative of a forearc wedge mantle origin. The Cr-magnetite rim contains inclusions of Cr-rich olivine ($\text{Cr}_2\text{O}_3 = 0.12\text{-}0.70 \text{ wt } \%$, $\text{Mg}\# = 0.950 \pm 0.004$, $\text{NiO} = 0.37 \pm 0.04 \text{ wt } \%$), in addition to Cr-rich antigorite ($\text{Al}_2\text{O}_3 = 0.5\text{-}3.1 \text{ wt } \%$, $\text{Cr}_2\text{O}_3 = 0.3\text{-}3.9 \text{ wt } \%$), diopside and brucite.

Formation of the Cr-rich olivine inclusions can be explained by dehydration of Cr-rich antigorite that developed around Cr-spinel grains. Slow diffusivity of Cr^{3+} compared to the olivine growth rate may have caused disequilibrium Cr incorporation into olivine under low-T conditions just above the $\text{Atg} + \text{Brc}$ breakdown equilibrium ($\sim 460\text{-}500 \text{ }^\circ\text{C}$). Alternatively, a distinct Cr substitution mechanism ($\text{Cr}^{3+} + \text{Fe}^{3+} = \text{Mg} + \text{Si}$) than that proposed for high-T olivine ($\text{Cr}^{2+} = \text{Mg}$ or $2\text{Cr}^{3+} + \text{vacancy} = 3\text{Mg}$) could explain the low-T formation of Cr-rich olivine. In any case, the local uptake of Cr in olivine from the Sanbagawa metaserpentinite does not imply very high-T conditions, and this weakens the main basis of the pseudotachylyte hypothesis for the spinifex-like textured peridotite in Cerro del Almirez. The geological record on the causal link between deserpentinization and deep earthquake nucleation remains elusive.

Keywords: Cr-rich olivine, antigorite, dehydration, subduction zone

振幅—継続時間スケーリングから推測される四国西部における深部低周波微動のスケール長の空間変化
Spatial variation in scale length of deep low-frequency tremor inferred from duration-amplitude scaling in western Shiko

堀野 一樹^{1*}; 平松 良浩²; 水上 知行²; 小原 一成³; 松澤 孝紀⁴

HORINO, Kazuki^{1*}; HIRAMATSU, Yoshihiro²; MIZUKAMI, Tomoyuki²; OBARA, Kazushige³; MATSUZAWA, Takanori⁴

¹ 金沢大学大学院自然科学研究科自然システム学専攻, ² 金沢大学理工研究域自然システム学系, ³ 東京大学地震研究所, ⁴ 防災科学技術研究所

¹Division of Natural System, Graduate School of Natural Science and Technology, Kanazawa University, ²School of Natural System, College of Science and Engineering, Kanazawa University, ³Earthquake Research Institute, University of Tokyo, ⁴National Research Institute for Earth Sciences and Disaster Prevention

Slip properties on plate interface vary largely along dip direction from seismic to aseismic slip. At the transition zone at depths of 25-35 km, non-volcanic deep low-frequency (DLF) tremor and short-term slow slip event occur in the Nankai subduction zone. Recent detailed studies (e.g. Obara, 2010) reveal along dip and along strike variations in the occurrence and the migration of DLF tremor in the transition zone. We report here an along dip variation in scale length of DLF tremor inferred from duration-amplitude scaling in the western Shikoku.

A physical process of natural phenomena is reflected by scaling law, for example, frequency of occurrence versus size distribution. Watanabe et al. (2007) reported that a duration-amplitude distribution of DLF tremor shows a better fit to the exponential model rather than the power-law model, which is different from regular earthquakes. We investigate the duration-amplitude distribution of DLF tremor using Hi-net data in the western Shikoku. The procedure of analysis is the same as that of Watanabe et al. (2007).

We focus on the slope of the exponential distribution for the duration-amplitude distribution of DLF tremor. The value of the slope is small in the western area and large in the eastern area. Noting along dip direction, we can recognize a weak variation of the value of the slope. Deeper DLF tremor tends to show a larger value of the slope than shallower DLF. A large value of the slope means a small scale length and vice versa.

Beneath the western Shikoku, the configuration and the age distribution of the subducting Philippine Sea plate changes significantly along the strike, generating a large variation in a thermal structure. Such a variation causes various modes of serpentinization in the hanging wall mantle. The resultant structures due to the different modes are the most likely cause of the detected transition of the scale length.

キーワード: 深部低周波微動, スケーリング則, 沈み込み帯, 規模別頻度分布, 蛇紋岩化

Keywords: deep low-frequency tremor, scaling law, subduction zone, size distribution, serpentinization